Proceedings of the 1996 IEEE International
Conference on Control Applications
Dearborn, MI • September 15-18, 1996

LONGITUDINAL HEADWAY CONTROL OF AUTONOMOUS VEHICLES

Cem Hatipoğlu†, Ümit Özgüner‡ and Martin Sommerville

Department of Electrical Engineering
The Ohio State University
Columbus OH 43210-1272
† *hatipo@ee.eng.ohio-state.edu* ‡ *ozguner.1@osu.edu*

Abstract

This paper is concerned with the development of a longitudinal controller for headway regulation of autonomous vehicles on highways. A supervisory hybrid controller is developed to switch between different control actions to implement a smooth intelligent cruise control (ICC) structure. Different decision regions are defined on the phase plane such that human driver actions are emulated as closely as possible. Hysteresis is introduced at the decision boundaries to avoid high frequency switchings from one controller to the other. Controllers with constant acceleration (or deceleration), smooth acceleration (or deceleration) and linear state feedback are studied and they are coordinated to efficiently implement ICC. A Kalman observer is employed to filter both the process and the measurement noise in the relative distance and relative velocity reading sensor (eg. laser range finder). The discrete states of operation are modeled for hybrid controller design and the conditions for transitions between those states are indicated. Simulation examples are provided along with some experimental results.

1. Introduction

In the past decade automation of highways has become an attractive field of research to use Advanced Vehicle Control Systems (AVCS). In general, studies on the design of autonomous vehicles involve the solution of two decoupled control problems: (i) The steering control (lane keeping), and (ii) The longitudinal (headway) control.

This paper exclusively focuses on the design of a longitudinal controller which can be used for ICC and/or platooning purposes. Three different control actions are studied and switchings between these controllers are coordinated accordingly to develop a single control algorithm that imitates the behavior of a typical driver. The designed controller uses local information, namely the separating distance and the relative velocity between the controlled vehicle and the leading vehicle, and generates the reference acceleration which is integrated and fed to the speed controller.

The speed control hardware developed at the Ohio State University (OSU) Center for Intelligent Transportation Research (CITR) has already been reported elsewhere, [1]. The tracking efficiency of this controller will be verified next, before presenting the major work of this paper. the speed controller, itself, is a supervisory controller which commands to the throttle and brake actuators to achieve the desired longitudinal speed. It involves detailed modeling of engine, transmission, torque converter, throttle actuator and brake actuator. Interested readers are referred to [3] for more detailed information on the development of the model and the hardware.

The control law is derived such that the separating distance, and the relative velocity between the two vehicles are smoothly forced towards the origin on the phase plane while maintaining the bounds on the longitudinal acceleration and deceleration rates and avoiding high frequency switchings at or around the destination point as well as the decision boundaries. A Kalman filter is employed to get rid of the process and measurement noise in the sensor readings as efficiently as possible.

The organization of the paper is as follows: The next section overviews the longitudinal car model. Section 3 states the ICC problem in the highway framework and studies the suggested controllers. Section 4 is devoted to Kalman filter design for state observation. The hybrid model of the ICC is provided in Section 5. Some simulation results are provided in Section 6. Section 7 provides preliminary experimental results. Finally, Section 8 is devoted to some concluding re-

0-7803-2975-9/96/$5.00 © 1996 IEEE

marks.

2. Longitudinal Car Model Overview

A car model for longitudinal dynamics consists of submodels of engine, torque converter, transmission, brake and vehicle body dynamics. Dynamics associated with the indicated subblocks are relatively sophisticated and are partially neglected for most applications. However, for precise speed control which will be used with ICC, each and every unit must be modeled. Figure 1 depicts an overview of the model. On this figure α is the throttle angle, ω_e is the engine rotational speed, T_t, T_p and T_s are the turbine, pump and shaft torques respectively, ω_t and ω_v are the turbine rotational speed and vehicle velocity respectively.T_b is the brake torque, and P_b is the brake unit line pressure. In previous studies [1], [3], a speed controller has been developed which generates inputs to the throttle and brake actuators such that the desired velocity can be achieved over a wide range of longitudinal velocities. The controller has been applied to a 1992 Honda Accord EX for experimentation. Details of the multi level speed controller can be found in [1].

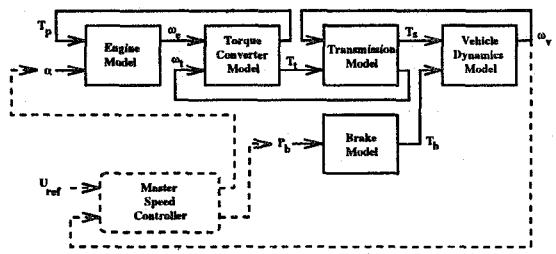

Figure 1: Longitudinal Vehicle Model

When the speed controller is embedded into the longitudinal car model, closed loop vehicle dynamics turn out to be relatively simple due to the efficiency of the lower level controllers. Based on the experimental data, it is assumed that if the physical limits on the vehicle performance are met, the speed controller will track the desired velocity profile perfectly. It should be noted that emergency maneuvers are not considered in this paper. Our motivation is to develop a multi-level controller for automatic longitudinal control for headway regulation. Since ICC and platooning are the possible applications for this study, passenger safety and drive comfort are considered as the prime concern in the design phase. In this paper the longitudinal acceleration and deceleration of the vehicle will be considered bounded. Let a_m be the longitudinal acceleration of the controlled vehicle at a given time instant. Then,

$$-D_{max} \leq a_m \leq A_{max} \qquad (1)$$

where $D_{max} > 0$ and A_{max} are the maximum deceleration and acceleration rates of the vehicle respectively.

The primary objective of the controller studied in this paper is to synthesize the desired velocity for the speed controller based on the sensor inputs regarding the relative velocity and relative distance with respect to the leading car. The hybrid supervisory controller will be analyzed primarily for ICC development which can be easily modified for platooning applications. Note that more emphasis will be given to ICC studies in this paper.

3. Problem Statement & Controller Development

Our objective is to come up with a hybrid model for ICC together with the decision rules which automate the longitudinal motions of a cooperative vehicle. Consider Figure 2.

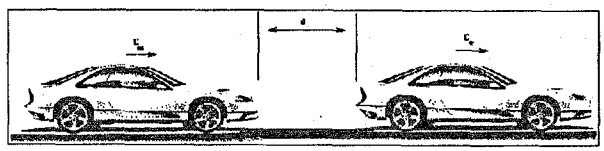

Figure 2: Vehicle Following Scenario

The dynamics of the relative velocity ΔU and the relative distance Δd are given as:

$$\Delta \dot{d} = -\Delta U \qquad (2\text{-a})$$

$$\Delta \dot{U} = a_{ref} - \dot{U}_c \qquad (2\text{-b})$$

where $\Delta U = U_m - U_c$. U_c is the leading car's longitudinal velocity, and a_{ref} is the reference acceleration.

The highway safety distance, d_{safe} is defined as a function of the operating velocity as follows:

$$\Delta d_{safe} = \tau U_m + \Delta d_o \qquad (3)$$

where τ is given in terms of seconds, and d_o in meters. Define $\widetilde{\Delta d} = \Delta d - \Delta d_{safe}$.

The performance of the master speed controller is shown on Figure 3. The following observations are made:

- There is almost perfect tracking during the breaking regions up to deceleration rates of $0.2g$ m/s^2 where g is the gravitational acceleration.
- Tracking is fairly reasonable during acceleration too. However, although the vehicle handles $0.1g$ acceleration rate up until $40mph$, it can not accelerate quicker than $0.05g$ when traveling at velocities higher than $40mph$ due to engine power limitations,

- As long as physical limits of the vehicle (acceleration/deceleration rates) are considered, MSC manages to track constant acceleration trajectories relatively well. For this particular experimental vehicle, we will let $D_{max} = 0.1g\ m/s^2$ and $A_{max} = 0.05g\ m/s^2$ in controller design phases and also in simulations.

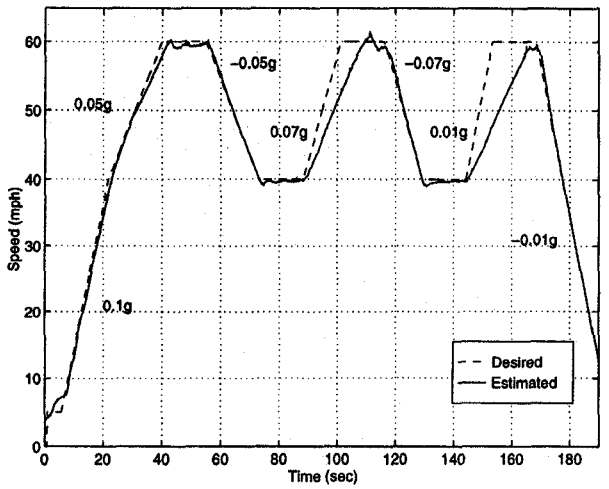

Figure 3: Performance of the Master Speed Controller

In the following sections different control strategies will be considered to regulate the relative velocity and relative distance between adjacent vehicles to desired values.

3.1. Constant Acceleration/Deceleration

Assume a constant acceleration (deceleration) scenario solely for analysis purposes. Assume $\Delta\dot{U} = a_{const}$. If the leading vehicle is traveling at a constant speed, i.e. $\dot{U}_c = 0$, then $\dot{U}_m = \Delta\dot{U} = a_{const}$. Constant acceleration/deceleration curves are parabolic on the phase plane satisfying the equation:

$$\widetilde{\Delta d} = \frac{1}{2a_{const}}\Delta U^2 - \frac{1}{2a_{const}}\Delta U \Delta U_o + \Delta d_o \quad (4)$$

where ΔU_o and Δd_o denote the initial conditions on the phase plane. Note that the parabola corresponding to the maximum deceleration rate determines a region beyond which the longitudinal controller (without emergency steering maneuvers) is not sufficient to avoid collision. The area

$$\Delta U \geq \sqrt{2D_{max}\left(\widetilde{\Delta d} - \tau U_m - \Delta d_o\right)} \quad (5)$$

for $\widetilde{\Delta d} \geq \tau U_m + \Delta d_o$ defines the region where collision is inevitable even if the vehicle decelerates at the maximum allowed rate. $\widetilde{\Delta d} < \tau U_m + \Delta d_o$ is the collision region.

3.2. Smooth Acceleration/Deceleration

On the $(\widetilde{\Delta d}\ ,\ \Delta U)$ phase plane, if the vehicle is operating in the first or third quadrants it is possible to direct system trajectories towards the origin on a straight line. The desired acceleration is determined by the following equation:

$$\frac{\frac{d(\Delta U)}{dt}}{\frac{d(\widetilde{\Delta d})}{dt}} = \frac{\Delta U}{\widetilde{\Delta d}} \quad (6)$$

Since $d(\Delta U)/dt = a_m - \dot{U}_c$ and $d(\widetilde{\Delta d})/dt = -\Delta U$, the reference acceleration for the controlled car is found to be,

$$a_f = -\frac{\Delta U^2}{\widetilde{\Delta d}} + \dot{U}_c \quad (7)$$

When this approach is used, the system trajectories satisfy:

$$\Delta U = \Delta U_o e^{-\frac{\Delta U_o}{\widetilde{\Delta d_o}}t} \quad (8\text{-a})$$

$$\widetilde{\Delta d} = \widetilde{\Delta d_o} e^{-\frac{\Delta U_o}{\widetilde{\Delta d_o}}t} \quad (8\text{-b})$$

This approach works well, and ensures the convergence to the origin simultaneously from any initial point on the I. and III. quadrants. However, it should be noted that the rate of convergence to the origin is a function of the initial condition which may be arbitrarily small or large. This problem should be remedied separately with the introduction of appropriate decision boundaries which is the concern of Section 5.

3.3. Linear Control Region

A linear region around the origin was chosen to avoid limit cycles (Same observation on this can be found in [4]). To avoid uncomfortable jerky behavior caused by oscillations around the destination point, an elliptic region is defined around the origin where a linear controller is employed. The interior of ellipse is parameterized by:

$$\frac{\Delta d^2}{\gamma^2} + \frac{\Delta U^2}{\sigma^2} \leq 1 \quad (9)$$

where $\pm\gamma$ and $\pm\sigma$ define the ellipse's $\widetilde{\Delta d}$-axis and ΔU-axis crossings respectively. Within this region a linear state feedback control law of the form $a_m = -\kappa_1\widetilde{\Delta d} - \kappa_2\Delta U$ is used. Consequently the closed loop system dynamics are described by,

$$\dot{\widetilde{\Delta d}} = \tau\kappa_1\widetilde{\Delta d} + (-1 + \tau\kappa_2)\Delta U \quad (10\text{-a})$$

$$\Delta\dot{U} = -\kappa_1\widetilde{\Delta d} - \kappa_2\Delta U - \dot{U}_c \quad (10\text{-b})$$

The feedback gains, namely κ_1 and κ_2, have to be chosen such that the closed loop system poles are on the

open left half plane (LHP) which guarantees asymptotic stability. The closed loop poles are found from the zeros of the following equation:

$$s^2 + (\kappa_2 - \tau\kappa_1)s - \kappa_1 = 0 \qquad (11)$$

For experiments $\kappa_1 = -0.4$ and $\kappa_2 = 2$ were picked. For $\tau = 1sec$ closed loop poles are at $s_1 = -2.2$ and $s_2 = -0.2$ which are experimentally observed to perform well.

Define $\rho = \max(D_{max}, A_{max})$. It is found that when the elliptic region is defined for the linear controller, if the following condition is satisfied, unnecessary switchings between the linear and nonlinear controllers will be avoided:

$$\gamma \geq \frac{\sigma^2}{\rho} \qquad (12)$$

4. Kalman Filter Design

The above controllers all require both the relative velocity and the relative distance information. A laser rangefinder is being used to obtain these data. Since the laser range finder used only provides distances and velocities at quantized levels (integer multiples of its resolution), these measurements were not precise. The laser range finder has a maximum resolution of $0.2m$ in distance measurement and $1km/hr$ in relative velocity measurement. To avoid discrete jumps due to the quantized sensor readings, a Kalman Filter was designed to estimate Δd and ΔU given the laser rangefinder data. A sampled data system model with the sampling time of T seconds is considered. The relative distance and relative velocity are modeled as:

$$\begin{bmatrix} \Delta d_{k+1} \\ \Delta U_{k+1} \end{bmatrix} = \begin{bmatrix} 1 & T \\ 0 & 1 \end{bmatrix} \begin{bmatrix} \Delta d_k \\ \Delta U_k \end{bmatrix} + G\Omega_k \qquad (13)$$

where Ω_k models the process noise, namely the velocity variance of the leading car which is multiplied by the input gain matrix $G \in \mathcal{R}^{2\times 1}$. We also model the measurement noise:

$$\begin{bmatrix} \overline{\Delta d}_k \\ \overline{\Delta U}_k \end{bmatrix} = \begin{bmatrix} \Delta d_k \\ \Delta U_k \end{bmatrix} + \begin{bmatrix} \xi_k \\ \zeta_k \end{bmatrix} \qquad (14)$$

where ν_k=$[\xi_k\ \zeta_k]^T$ is the noise term, and $\overline{\Delta d}$ and $\overline{\Delta U}$ represent the sensor outputs.

Both Ω_k and ν_k are assumed to be zero mean with covariances $\mathcal{Q}$ and $\mathcal{R}$ respectively. The covariance of the measurement noise $\mathcal{R}$ is easily determined from experimental data, however the process noise covariance $\mathcal{Q}$ and the multiplicative gain matrix G are not easy to obtain. They are determined by iterative tuning on an initial random selection. Let the error covariance matrix at the k^{th} sample be denoted by P_k. Then,

$$P_{k+1} = [P^-_{k+1} + C^T R^{-1} C]^{-1} \qquad (15\text{-a})$$

$$P^-_{k+1} = AP_kA^T + GQG^T \qquad (15\text{-b})$$

The best filter gain L is given by,

$$L = P_{k+1}C^T R^{-1} \qquad (16)$$

As can be seen, the filter gain is time varying in general. It was observed that for this particular application the steady state value of this error covariance matrix can be used instead of the time varying gain matrix. This approximation eliminates various time consuming calculations involving matrix inversions and recursions, which shortens the processing time. Once the steady state value of the error covariance matrix $P = \lim_{k\to\infty} P_k$ is determined, the filter gain L becomes constant. The resulting Kalman filter is in the following form:

$$\begin{bmatrix} \widehat{\Delta d}^-_{k+1} \\ \widehat{\Delta U}^-_{k+1} \end{bmatrix} = \begin{bmatrix} 1 & T \\ 0 & 1 \end{bmatrix} \begin{bmatrix} \widehat{\Delta d}_k \\ \widehat{\Delta U}_k \end{bmatrix} \qquad (17)$$

$$\begin{bmatrix} \widehat{\Delta d}^+_{k+1} \\ \widehat{\Delta U}^+_{k+1} \end{bmatrix} = \begin{bmatrix} \widehat{\Delta d}^-_{k+1} \\ \widehat{\Delta U}^-_{k+1} \end{bmatrix} + L\left(\begin{bmatrix} \overline{\Delta d}^-_{k+1} \\ \overline{\Delta U}^-_{k+1} \end{bmatrix} - \begin{bmatrix} \widehat{\Delta d}^-_{k+1} \\ \widehat{\Delta U}^-_{k+1} \end{bmatrix} \right)$$

The following numerical values are used for the filter in experiments:

$$\mathcal{R} = \begin{bmatrix} 0.0716 & 0.0084 \\ 0.0084 & 0.0563 \end{bmatrix} \qquad G = \begin{bmatrix} 0.1 \\ 1.0 \end{bmatrix}$$

$$P = \begin{bmatrix} 0.00203 & 0.00236 \\ 0.00236 & 0.00427 \end{bmatrix} \qquad L = \begin{bmatrix} 0.00239 & 0.03829 \\ 0.02449 & 0.07219 \end{bmatrix}$$

and, $\mathcal{Q} = 1$, $T = 0.01sec$, $C = I_{2\times 2}$. The update law on the Kalman filter is turned off when the laser range finder does not find a target ahead.

5. Hybrid Modeling & Decision Boundaries

ICC is an excellent example for a hybrid system with a continuous state system (the vehicle) that operates under different control laws which form a finite discrete set. While implementing ICC, the longitudinal velocity of the vehicle is controlled by either of the three control methods (constant acc./dec.; smooth acc./dec.; linear controller) or no action is taken. The decision boundary selection for the controller switchings are the major task in the implementation phases. It is observed that people have different habits of driving, hence different decision characteristics. The limitations of the vehicle in terms of acceleration/deceleration characteristics constitute stiff boundaries for the controller. Yet many people restrict their driving to a subset within those limitations. Although people drive differently, it is believed

that the response of a driver can be parameterized in terms of preferred acceleration, deceleration rates and response times. At the present time, studies are underway regarding this parameterization and the related hybrid formulation.

5.1. Smooth Dec./Acc. Control

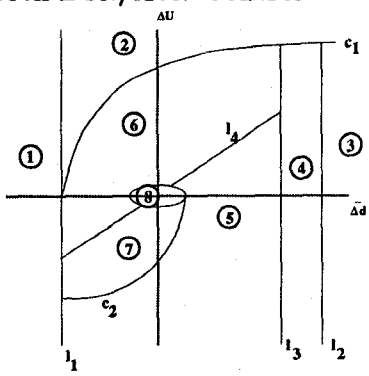

Figure 4: Control Scheme I

Consider Figure 4. There are 8 regions bounded by lines/curves other than the axes. c_1 and c_2 are the parabola defined by the maximum deceleration and maximum acceleration rates of the vehicle respectively. l_1 is the collision boundary. l_2 defines the range of the sensor system. l_3 is a user defined action boundary. The slope of l_4 determines the lower bound for the convergence rate to the origin. *Region 1* describes a collision, *Region 2* is the portion of the phase plane where collision can not be avoided even if the vehicle slows down at the maximum deceleration rate without advanced emergency steering maneuvers. While in this region, the vehicle should provide noticeable emergency warning to the driver. *Region 3* defines the limits of the sensor system. Since no vehicle/obstacle is detected in the sensor range, ICC acts like a conventional cruise control unit and maintains the set speed U_{set}. *Region 4* is where the sensors start detecting an obstacle but no action is taken either because it is still far away or for sensor fault detection purposes. If the vehicle enters *Region 6* (*Region 7* resp.), then the smooth acceleration/deceleration control law of Section 3.2 is employed until the system trajectories enter either Region 8 (Region 8 resp.) or $\widetilde{\Delta d}$ becomes negative (positive resp.). If the second condition occurs the vehicle is decelerates (accelerates resp.) at the maximum rate until it enters Region 8 (Region 8 resp.) or Region 7 (Region 5 resp.). If in *Region 5*, the vehicle is accelerated at maximum rate until the trajectories enter Region 6. In *Region 8*, the linear controller (as described in Section 3.3) is employed. ICC is terminated whenever the controlled vehicle's speed tends to exceed the initial set speed and conventional cruise control is resumed. A small hysteresis is used while determining the slope of l_4 to avoid high frequency switchings between controllers.

6. Simulations

The simulation models of the vehicles, sensors and the controller have been implemented in Simulink using Matlab. Various different simulation examples were studied to test the performance of the designed controller. In this paper we would like to present a simulation example which demonstrates a very common scenario on highways: Cut-ins from arterials. This is when a vehicle merges between the leading vehicle and the controlled vehicle. Instantaneously there occurs a step change in the distance information falling far below the desired safety distance. In most of the cases the new car's velocity is slower than that of the previous leader initially. In this simulation example, it is assumed that the leading vehicle travels at a constant longitudinal speed of $20m/s$ (45mph), and the initial velocity of the controlled vehicle is $25m/s$ (56.25mph). Initially, vehicles are separated by $50m$. At $t = 80sec$, a new vehicle cuts inbetween the two vehicles instantaneously dropping the separating distance to $10m$. The vehicle is assumed to speed up from $18m/s$ (40mph) to $24m/s$ (54mph) at a rate of $0.1m/s^2$. The acceleration of the leading vehicle is assumed not known. Gaussian measurement noise is considered for Δd and ΔU measurements. There is a first order unmodeled actuator dynamics. $\tau = 1sec$ and $d_o = 1m$. The simulation results are shown on Figures 8 and 7.

7. Experimentation/More Simulation

We have performed a series of experiments using this controller design. For safety purposes, the initial experiments were conducted with the lead car being "virtual" (i.e. generated on a computer). The relative distance and the relative velocity information are extracted from calculations of the "Virtual car" simulation. From the follower point of view, this scenario is very similar to the actual scenario using real

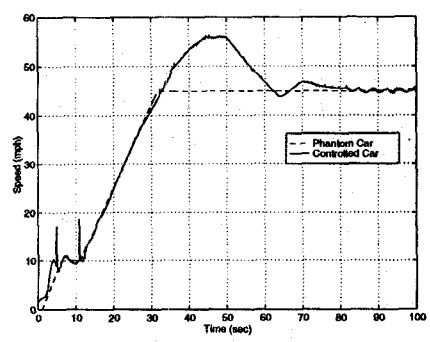

Figure 5: Exp: Relative Velocity

cars with the main difference being more noise free information regarding the lead car. The studied scenario is as follows: The virtual car is accelerated to $45mph$ and its velocity is kept at that level thereafter. Meanwhile the follower is accelerated to $55mph$ until the two vehicles are separated by about $200ft$. Then it maintains its speed until it enters the action region (around $130ft$ separation). Later, it smoothly decelerates to match its speed to that of its leader's while achieving the desired safety distance. See Figures 5 and 6.

8. Conclusions

In this paper we have explained a longitudinal controller for headway regulation for ICC applications which can be easily modified for platooning purposes as well. An overview on longitudinal car modeling is followed by the ICC problem. Three different control actions are studied and the hybrid system modeling problem is introduced along with the description of the suggested decision boundaries that yields the desired characteristics of ICC while satisfying passenger safety and drive comfort. A simulation example is introduced and an experimented scenario is presented.

9. Acknowledgment

The authors gratefully acknowledge the support by the Center for Intelligent Transportation Research (CITR) of OSU.

References

[1] M. Sommerville, K. Redmill, and Ü. Özgüner, "A Multi-Level Automotive Speed Controller", SAE Paper 961011, presented in SAE '96, Detroit, MI.

[2] Ü. Özgüner, C. Hatipoğlu, K. A. Ünyelioğlu, J. Young, L. Henderson, and S. Drakunov "Headway and Steering Control of Truck Platoons Based on a Radar Sensor", *Proceedings of ITS-America meeting '96*, Houston, TX.

[3] M. Sommerville, "Implementation of a Longitudinal Controller for use on an Automated Highway System", *Master's Thesis*, the Ohio State University, Dept. of Electrical Engineering, 1996.

[4] J. G. Bender, "Experimental Studies in Vehicle Automatic Longitudinal Control", *Master's Thesis*, the Ohio State University, Dept. of Electrical Engineering, 1968.

[5] S. Germann and R. Isermann, "Modeling and Control of Longitudinal Vehicle Motion", *Proceedings of the ACC*, pp 1-5, 1994.

[6] D. H. McMahon, V. K. Narendra, D. Swaroop, J. K. Hedrick, "Longitudinal Vehicle Controllers for IVHS: Theory and Experiment", *Proceedings of the ACC*, pp. 1753-1757, 1992.

[7] P. Ioannou, Z. Xu, D. Clemson and T. Seija, " Intelligent Cruise Control: Theory and Experiment", *Proceedings of 32nd CDC*, pp. 1885-1890, 1993.

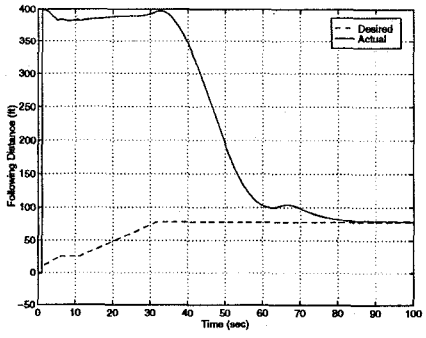

Figure 6: Exp: The Separating Distance

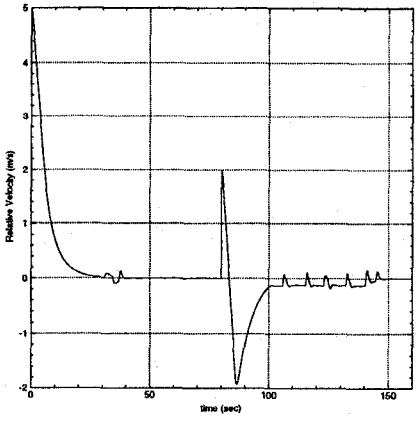

Figure 7: Sim: Relative Velocity

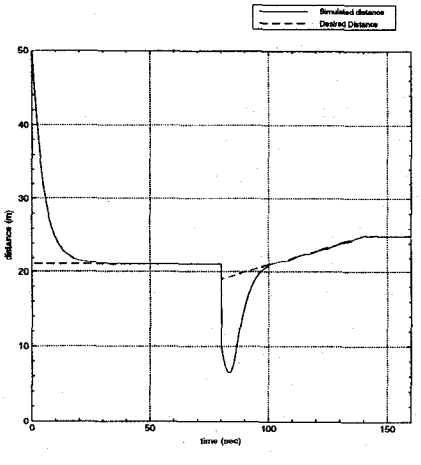

Figure 8: Sim: The Separating Distance